UNCONVENTIONAL RESOURCES TECHNOLOGY CONFERENCE
FUELED BY SPE • AAPG • SEG

URTeC:2882313

Case study: Casing Deformation Caused by Hydraulic Fracturing-Induced Fault Slip in the Sichuan Basin

Zhaowei Chen[1], Lang Zhou[2], Rall Walsh*[3], Mark Zoback[4];
1. CNPC Engineering Technology R&D Company Limited, 2. Petrochina Southwest Oil & Gas Field Company, 3. Decision Geomechanics LLC，4. Stanford University

Abstract

Out of the 101 wells in the Changning and Weiyuan shale gas blocks in Southwest China's Sichuan basin drilled before March 2016, casing deformation occurred in 32. Analysis of one of these wells shows a fault at a sheared casing location, which suggests that hydraulic fracturing-induced fault shear is likely the cause of casing deformation. Here, we present a probabilistic geomechanical model evaluating imaged faults. The fact that the deformed casing is found close to a fault zone indicates that casing deformation was caused by hydraulic fracturing-induced fault slip. From the microseismic monitoring data, we can determine the strike and dip of the fault: N57°E and 70°. Image and wireline log data, as well as mini-frac test data from the subject well and other nearby wells, can be used to constrain geomechanical parameter distributions. Using these parameters, Mohr-Coulomb fault activation was evaluated. A Quantitative Risk Analysis (QRA) was undertaken to analyze both the probability of induced fault slip and the sensitivity of the slip to model parameters. Finally, we repeat this analysis for each fault interpreted from an ant tracked image, where each fault is colored by its potential for induced slip under the same pressure.

The results show that, under current in-situ stress conditions, faults in the block are critically stressed and easily activated. After propagating uniformly distributed uncertainties in the geomechanical model using Monte Carlo simulation, we can observe that the fault that sheared had a 70% probability of doing so under a pressure increase of 2,500 PSI. Applying this analysis to mapped faults allows us to separate fault segments into those which should ideally be avoided by future production wells (red), and those which appear stable (green). The uncertainty analysis can also be used to prioritize further data collection by focusing on the parameters that the answer is most sensitive to (in this case S_{hmin} and the natural pore pressure). The procedure highlighted herein provides a method for understanding the causes of casing deformation as well as measures for mitigating fault activation. It also shows the importance of seismic data - the same well appears to cross a second critically stressed fault which did not respond seismically as would be indicated by microseismicity or a sheared casing.

Introduction

In the Changning-Weiyuan national shale gas demonstration area of the Sichuan Basin, China, commercial shale gas production has been realized by using hydraulic fracturing to improve reservoir interconnectivity and permeability. Casing deformation is a significant challenge encountered in shale gas production in this play. Between the beginning of 2009 and March of 2016, 47 points of casing deformation occurred in 32 of 101 wells (of which 90 are horizontal). This resulted in the improper setting of bridge plugs and a decrease in the number of fracturing stages. The resulting operational difficulties made it difficult to ensure wellbore integrity and manage risk. The reduction in the number of fracturing stages led to lower well production, poor wellbore integrity, and a shortened well lifespan. These factors materially inhibit the economics of shale gas production in the basin. Here,

we combine seismic data with geomechanics techniques to analyze casing deformation events induced by hydraulic fracturing.

Observation of casing deformation

The Ning 201-1H well (Figure 1) drilled in 2012, was the first horizontal shale gas well in the Changning block of the Sichuan Basin. The well's TVD is 2500 m, and its TD is 3790 m. The lateral length is 1452 m, the maximum deviation is 96.28°, and the azimuth is 7.1°. The diameter of the horizontal wellbore is 21.59mm. The outer diameter and the width of casing of the horizontal section were 139.7 mm and 9.17 mm, respectively. Multi-stage hydraulic fracturing was conducted from toe to heel by a cable-conveyed cluster perforation and bridge plugging system. A smooth wiper trip was completed before fracturing began.

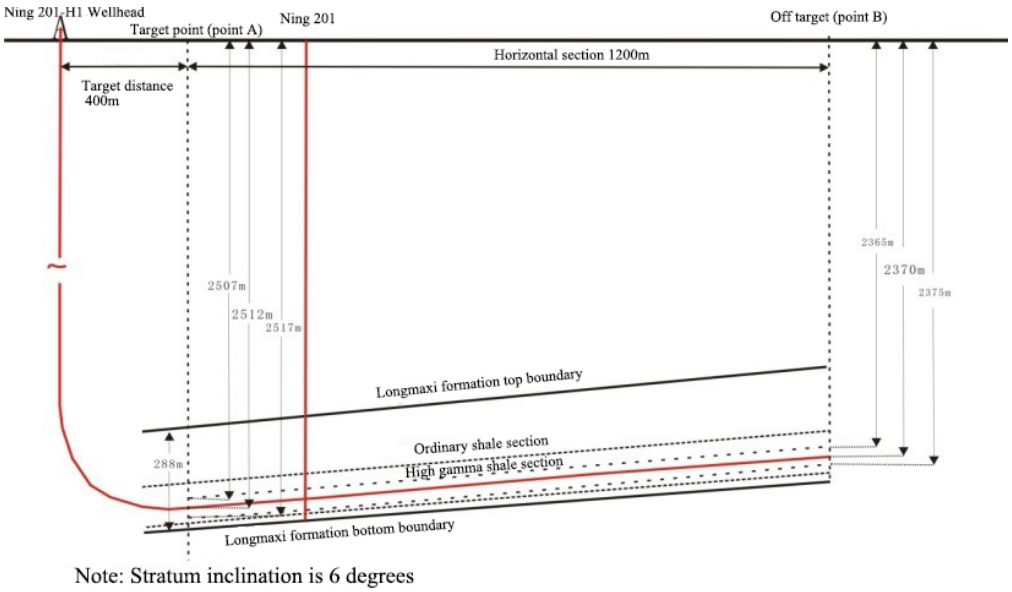

Figure 1: Trajectory of the Ning 201-1H well, drilled in the Sichuan basin in 2012.

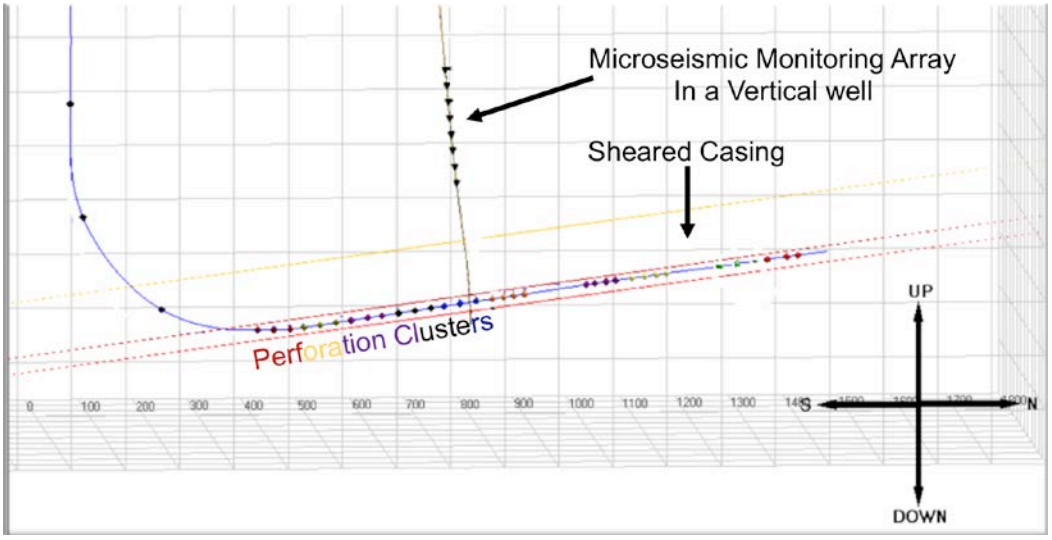

Figure 2: Perforation clusters and the micro-seismic monitoring array

Microseismic monitoring was conducted in Ning 201, which is an offset vertical well (Figure 2). Eight receivers were used; the lowest was at a depth of 2305 m deep. Twelve stages were designed with a section length of 75-100m; 3-4 perforation clusters were used per stage. After the successful fracturing of the first and second stage, the number 2 bridge plug was pumped over and encountered resistance at 3490m. After taking out the bridge plug, coiled pipe and a 114.3mm mill shoe were used to pass through the well; these also became stuck at 3490 m. Scratches observed on the milling cone when it was removed suggest casing deformation (Figure 3). After milling cone removal, a bridge plug was set at the deformation location (3491 m). Table 1 shows planned and actual perforation locations.

Figure 3: Scratches on the milling cone, a preliminary indicator of a sheared casing.

24-arm caliper logging with a Multifinger Imaging Tool (MIT) was conducted for 3 offset wells; the measured deformation shape is similar to that shown for a different well in Figure 4. The deformation is convex-concave or S-shaped, indicating that the casing experienced shear deformation. Deformation caused the average inner diameter to decrease by 5-10mm. In the axial direction, the deformation spans about 1 meter. Shear deformation is typically caused by fault slip; all available information indicates that this was the case for the wells in question.

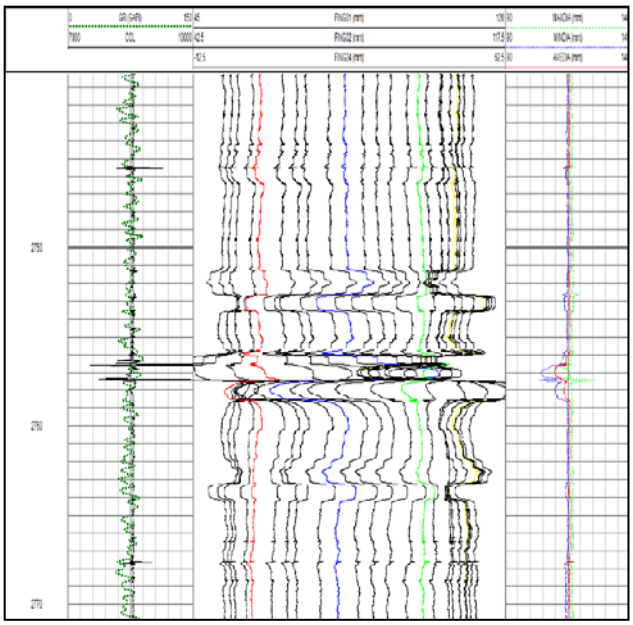

Figure 4: MIT caliper logs of a well in the Sichuan Basin (Chen, et al. 2017). The convex/concave, or S-shaped, deformation is indicative of sheared casing.

Observation of Faulting

The microseismic monitoring data in Figure 5 show that a high-intensity microseismic event cloud was produced by fracturing the first stage. In all the subsequent stages, microseismic events continued extending this cloud. The cloud can be interpreted either as an open natural fracture zone or a small fault. We estimated the strike of the fault to be N57°E; the dip was around 70 degrees. The fault has a length of about 860 m and a height of about 290 m. Several magnitude 2+ events also occurred during stimulation. The casing deformation point is about 100m away from the fault indicated by the microseismic data. However, microseismic monitoring is carried out in a nearby vertical well labeled 201 in Figure 5, and is associated with large horizontal uncertainties. Therefore, it is reasonable to relate casing deformation to fault activation near the toe of the well.

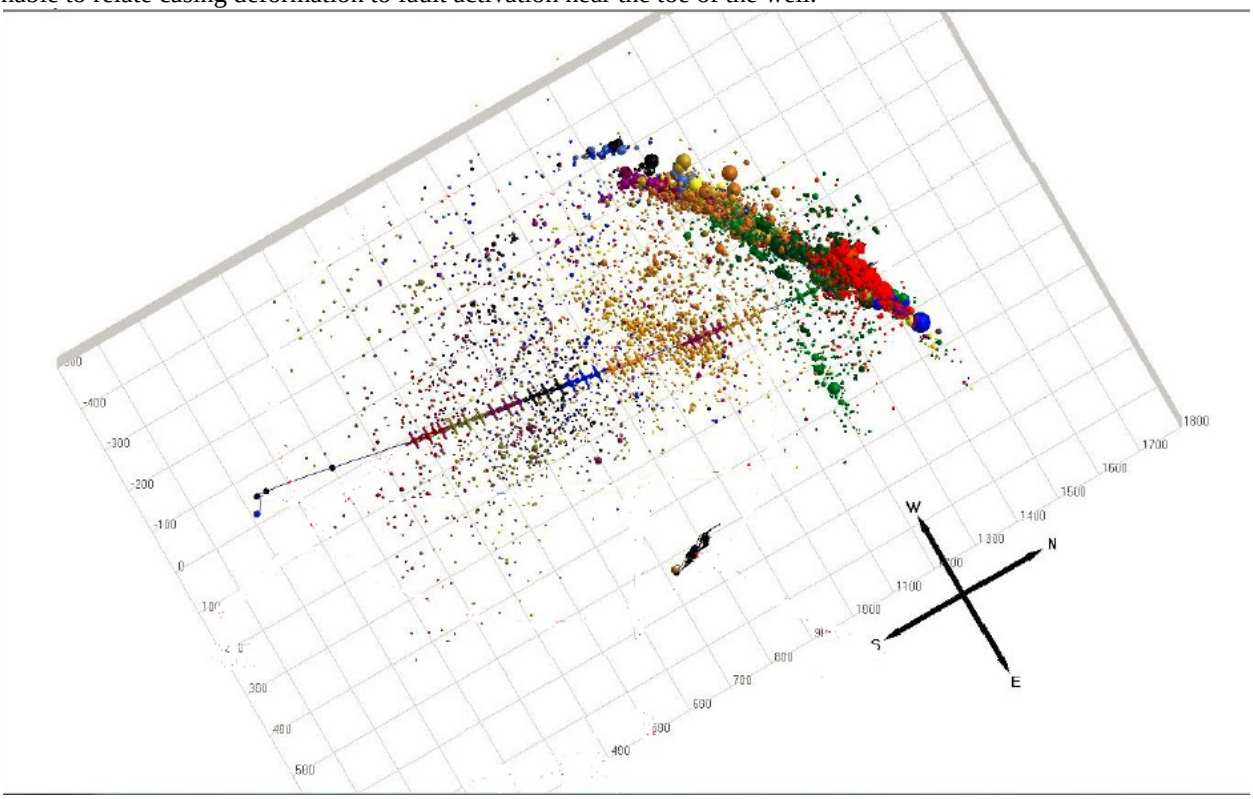

Figure 5: Top-down view of micro-seismic monitoring data

Ant tracking was used to analyze the faults in the Ning 201 block (Figure 6). We can see that the well crosses two faults - a small one by the toe of the well and a larger fault closer to the center of the well. Lack of casing deformation or microseismic observation suggest that the larger fault did not experience slip. It's plausible that the fault is at a different depth from the well and is therefore not intersected or stimulated. This underscores the importance of properly locating and imaging faults in geomechanical analyses. The smaller fault near the toe of the well strikes N57°E in the ant tracking image; this observation is in agreement with the microseismic cloud.

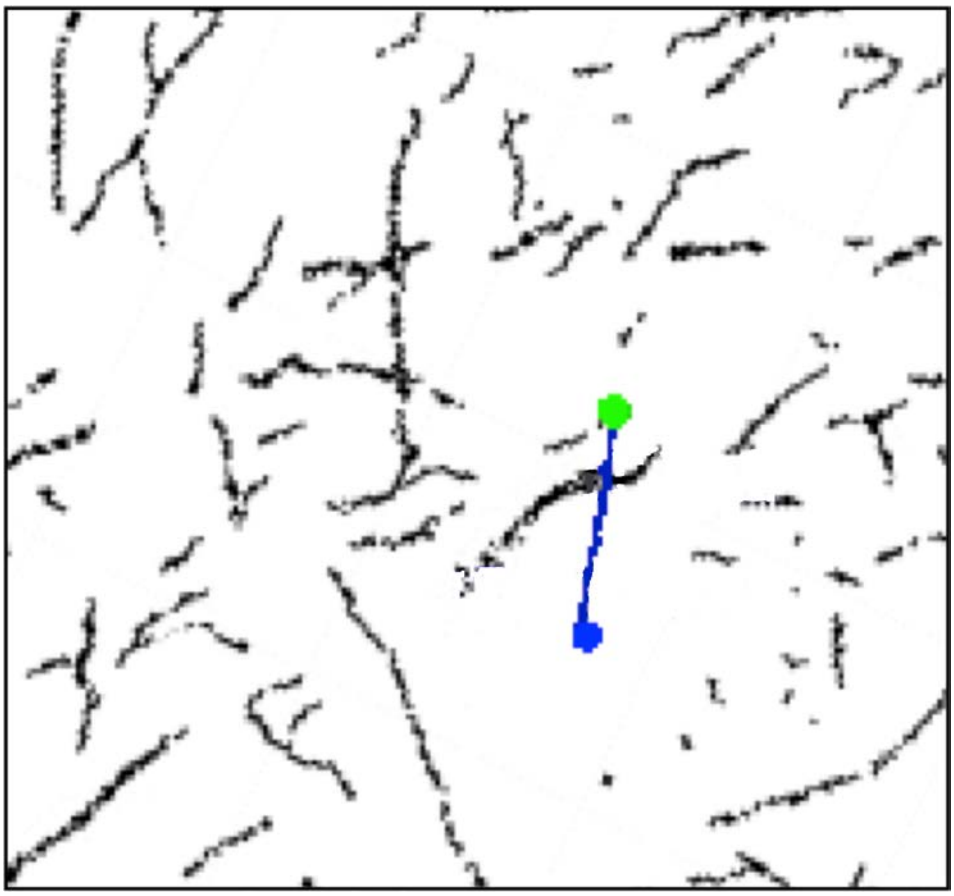

Figure 6: faults in the Ning 201 block, interpreted with ant tracking. The green dot is the toe of the well and the blue dot shows the heel and the wellhead.

Geomechanical Model

To build the geomechanical model, we first constrained the various relevant parameters and corresponding uncertainties (Zoback, 2010). The overburden constraints are based on density measurements, which were made between ~1600 m TVD and the TD of the well. We used an exponential curve to approximate density from ~50m to ~1600mTVD. The density curve shows values ranging from ~1.0g/cc at the ground surface to ~2.0g/cc at ~50m depth; these values are consistent with density measurements made in onshore environments in other regions. Pseudo-density data derived from sonic data are used for depths of ~1780 m to ~1850 mTVD. The density data were integrated to obtain a depth-continuous vertical stress profile.

Ning 203 is the offset vertical well in which the formation pressure tests were carried out. The natural formation pressure is 31.57MPa and the equivalent gradient is 1.4SG. S_{hmin} is constrained based on mini-frac data conducted in the Longmaxi Formation in the Ning 201 well. The Fracture Closure Pressure ranges from 6541-6596 psi; these values are based on three interpretation approaches. The estimated S_{hmin} is about 1.9 SG at a depth of 2439.5 mMD (2434.1 mTVD).

Continuous wellbore breakouts can be observed in Formation Micro Imager (FMI) data from the Ning 201 well. Based on wellbore failures observed in FMI data, we can infer that the azimuth of S_{Hmax} is approximately 109°N. The stress direction in the Changning field matches regional observations based on the world stress map. S_{Hmax} is constrained based on observed wellbore failures and knowledge of S_{hmin} and rock strength. Unconfine d Compressive Rock Strength (UCS) ranges from 65 – 75 MPa; there is a breakout width of 60° at ~2445m TVD. The magnitude of S_{Hmax} is 3.46 ± 0.14 sg. The Changning Field, therefore, appears to be associated with a strike-slip

stress regime (S_{hmin} < $S_{Vertical}$<S_{Hmax}). In our analysis, we used uniform geomechanical parameter distributions, as shown by the red distributions in Figure 7 and summarized in table 2.

Fault Activation Analysis

We applied Quantitative Risk Analysis (QRA), from the Probabilistic Geomechanics tab of the Fault Slip Potential program (Walsh et al. 2017), to analyze the stimulation-induced fault shear. By propagating uniformly distributed uncertainties in the geomechanical model through Monte Carlo modeling, we conclude that, prior to the event, the fault that sheared had a 70% probability of shearing with the addition of 2,500 PSI (the downhole pressure during stimulation, see Figure 8B). After completing the analysis, we apply it to the interpretation of an ant track image (Figure 8A). This allows future well siting in locations that minimize the potential for sheared casing (Figure 11). Figure 9 shows a sensitivity analysis of the geomechanical model, which allows for prioritization of data-gathering to better constrain the model and lower uncertainties associated with future decisions.

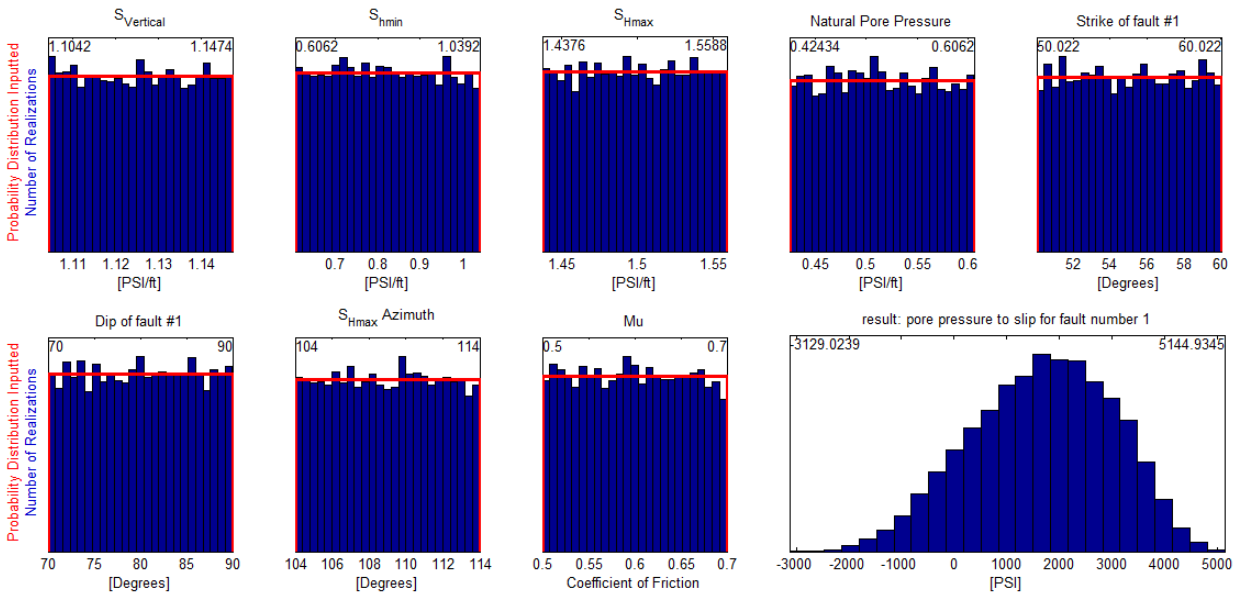

Figure: 7 Probabilistic distributions of geomechanical uncertainties for the fault that sheared during hydraulic fracture stimulation. The bottom right panel shows the resulting probabilistic distribution of pore pressures required for slip on fault number 1. This distribution is shown as a CDF curve in figure 8B.

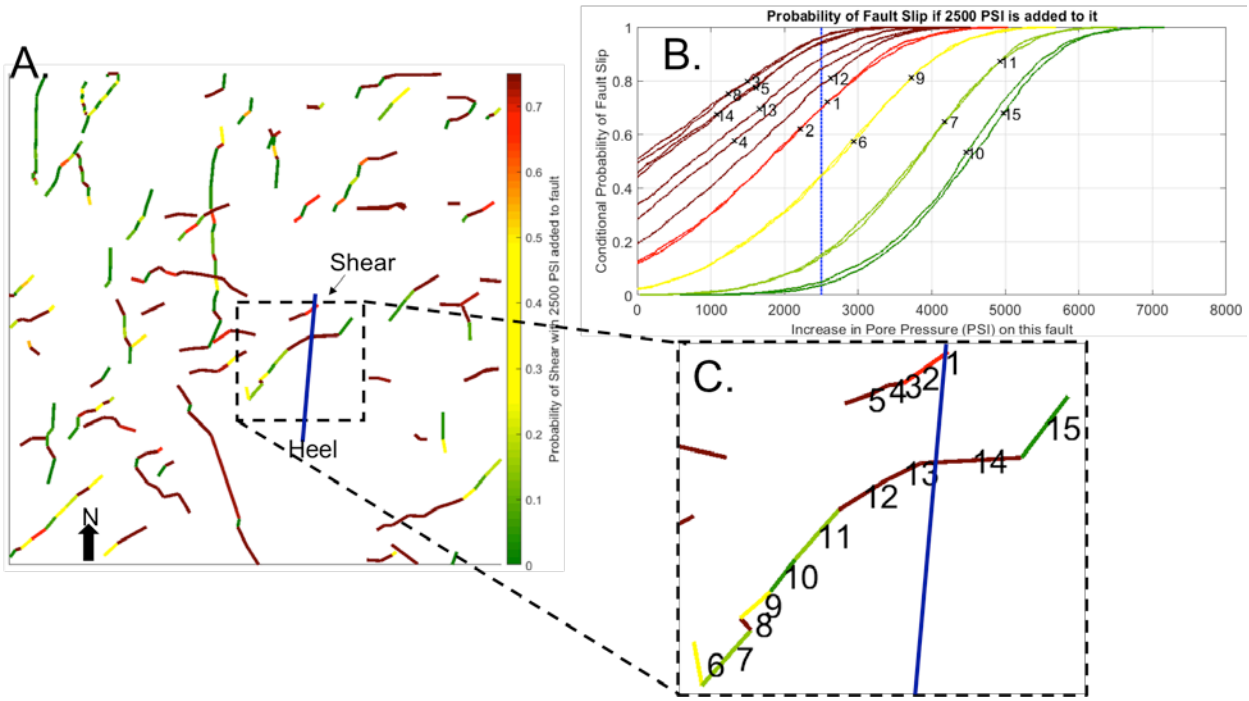

Figure 8A. An interpretation of the ant-tracked image (figure 6). We apply the probabilistic geomechanical model (as in Figure 7) to each fault segment and color it by its probability of induced fault slip under a stress increase of 2500 PSI. This interpretation can be used to site wells that don't intersect hazardous faults or to test the geomechanical model on other wells drilled within the block. Figure 8B: Probability of induced fault slip on numbered faults as a function of the total increase in pore pressure. 2,500 PSI (blue line) is the downhole pressure added during hydraulic fracture stimulation; this characterization assigns a 70% probability of slip to fault #1, meaning the fault would not have slipped under this pressure in only 30% of the possible models. Figure 10C: Map inset labeling fault segments as interpreted from Ant Tracking (corresponding to the CDFs in Figure 8B). The blue line shows the location of the Ning 201-1H well. Fault segment 13 appears in map view to be critically stressed, but it does not slip, possibly because it is at a different depth.

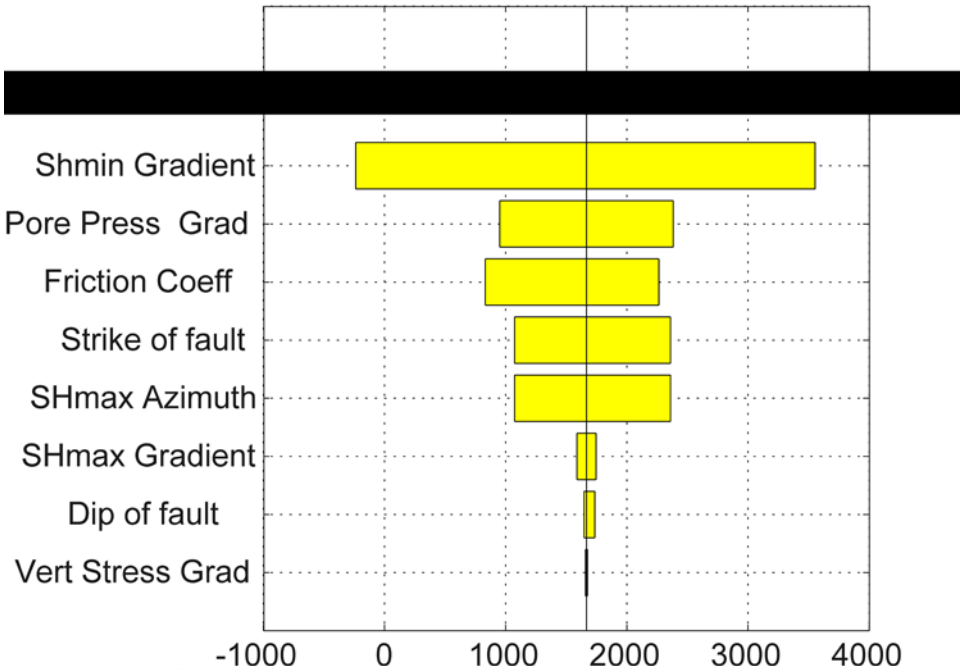

Figure 9: Sensitivity analysis results for Fault #1 can be used to prioritize data collection. Here S_{hmin} is the parameter that pore pressure to slip is most sensitive to.

Conclusion

Our results show which faults in the block are near critical stress states for current in-situ stress conditions. By propagating uncertainties in the geomechanical model using Monte Carlo modeling, we can conclude with hindsight that the fault that sheared had a 70% probability of doing with the addition of 2,500 PSI. Applying this analysis to mapped faults allows us to see which segments would ideally not be intersected by future production wells (red) and which pose less risk (green). Our uncertainty analysis can also be used to prioritize the most effective information-gathering techniques by focusing on the parameters that the answer is most sensitive to (in this case, S_{hmin} and natural pore pressure). The fact that the well crosses a fault that appears to be critically stressed but that did not slip highlights the importance of seismic data to the process of locating faults for geomechanical analysis. The procedure presented herein provides a framework for understanding and mitigating casing deformation events associated with fault activation.

Acknowledgments

Support was provided by the National Major Science and Technology Project “Factory drilling techniques and integrated application” (No. 2016ZX05022001), National Major Science and Technology Project “High efficiency and rapid drilling technology and equipment for deep and ultra-deep well” (No. 2016ZX05020002) , and Major Science and technology Project of CNPC “Research and application of key technologies for producing 30 billion cubic meters of natural gas in southwest oil and gas field” (No. 2016E-0612).

References

Zhaowei, Chen, Lin. Shi, Degui, Xiang. Mechanism and Countermeasures of casing deformation in Changning-Weiyuan shale gas demonstration area. Natural Gas Industry. 2016.36(11)

Walsh, R., et al. (2017) Fsp1.0: A program for probabilistic Estimation Of Fault Slip Potential resulting From Fluid Injection. A user guide available at SCITS.stanford.edu/software accessed 2/2018.

Zoback, M.D., (2010) Reservoir Geomechanics, Cambridge University Press.

Appendix A:

Table 1: Designed and Acutual Positions of Perforation Clusters

Stage	Designed			Actual		
	Stage section(m)	Perforation position (m)	Bridge plug position(m)	Stage section(m)	Perforation position (m)	Bridge plug position(m)
1	3663-3750	3745-3746 3724-3725 3677-3678	3671	3663-3750	3742.4-3743.0 3724.0-3724.7 3677.0-3677.7	3671
2	3583-3663	3656-3657 3619-3620 3586-3587	3577	3583-3663	3656.0-3656.7 3619.0-3619.7 3586.0-3586.7	3491

Table 2: 1D Geomechanical Model

Geomechanical Parameters	Low	High Value	Center	Plus/minus	Center PSI/ft	Plus/minus PSI/ft
S_{Hmax}	3.32 (SG)	3.6 (SG)	3.46 (SG)	0.14 (SG)	1.49818	0.06062
S_{hmin}	1.85 (SG)	1.95 (SG)	1.9 (SG)	0.05 (SG)	0.8227	0.02165
S_v	2.55 (SG)	2.65 (SG)	2.6 (SG)	0.05 (SG)	1.1258	0.02165
Pore pressure	0.99 (SG)	1.4 (SG)	1.19 (SG)	0.21 (SG)	0.51527	0.09093
Azimuth of S_{Hmax}	~104°	~114°	109	5		
Coefficient of friction	0.5	0.7	0.6	0.1		
Depth of calculation			2400m	0	7874 ft	0